Grain boundary engineering in a thermo-mechanically processed Nb-stabilized austenitic stainless steel

A Yunquera [1], D Jorge-Badiola [1], I Gutiérrez [1] and A Iza-Mendia [1]

[1] CEIT and Tecnun (University of Navarra), Donostia-San Sebastián, Basque Country, Spain

E-mail: djbadiola@ceit.es

Abstract. Three different thermo-mechanical strategies—annealing, strain recrystallization and strain annealing—were applied to a Nb-stabilized 304H austenitic stainless steel in order to study their effects on grain boundary character distribution (GBCD). An Electron Backscatter Diffraction (EBSD) analysis revealed specific combinations of cold reduction-temperature-time that favor annealing twinning. A uniform increase in microstructural size and special boundaries (particularly for $\Sigma 3$, $\Sigma 9$ and $\Sigma 27$ boundaries) was achieved under strain annealing conditions (low cold reductions) and long times at high temperatures ($\geq 990^\circ C$). These conditions provide a high fraction of special boundaries (about 80%), which replace the random grain boundary network and thus optimize the GBCD. The profuse presence of $\Sigma 3^n$ boundaries is attributed to the geometric interaction of twin-related variants during grain boundary migration. In addition to all this, precipitation takes place at the temperature range where optimum GBCD is achieved. The significance of precipitation in the different strategies was also tackled.

1. Introduction

Grain boundaries are crystallographic discontinuities where phenomena such as migration, sliding, solute segregation and precipitation can occur. However, some boundaries present special properties that improve material performance under the above mentioned degradation phenomena. The boundaries are usually described through the coincidence site lattice (CSL) model [1], which defines boundaries by the density of common sites (Σ) between grains sharing a boundary. Among all Σ boundaries, $\Sigma 3^n$ type boundaries are assumed to have a higher specialness, particularly $\Sigma 3$ boundaries. Within $\Sigma 3$ boundaries, many analyses have concluded that only $\{111\}$ plane-based $\Sigma 3$ boundaries, also known as coherent $\Sigma 3$ annealing twins, are special [2]. Thus, increasing the proportion of coherent $\Sigma 3$ boundaries by decreasing random High Angle Grain Boundaries (HAGB) is critical for obtaining grain boundary character distribution (GBCD) control and for improving intergranular properties. In that regard, Grain Boundary Engineering (GBE) aims to increase the density of special grain boundaries in materials with low SFE (stacking fault energy) through various thermo-mechanical routes that basically consist of applying a cold strain and following it with an annealing treatment [3,4]. Two types of GBE can be distinguished: strain recrystallization treatments that increase the proportion of special boundaries by forming new grains during recrystallization, and strain annealing treatments that promote high fractions of $\Sigma 3^n$ without forming new HAGB boundaries.

The excellent properties of austenitic stainless steels (ASS) under severe conditions make them an interesting objective for studying their behavior under supercritical conditions [5]. Over the last decade several studies have addressed GBE research on austenitic stainless steels [6,7]. More than 80% of special boundaries are obtained with strain annealing treatments [8,9]. Unlike previous studies, this study is focused on a Nb-stabilized 304H stainless steel, one of the materials likely to be employed under supercritical conditions, in which Nb(C,N) precipitation could play a role either as a microstructural controlling factor or as a matrix strengthener . The present study is intended to explore

and analyze the microstructures obtained when a Nb-stabilized 304H stainless steel is subjected to different final processing strategies that seek to achieve an optimum grain boundary network.

2. Experimental

The material used in this study is an 18Cr9Ni3CuNbN austenitic stainless steel. Various series of thermo-mechanical processes, whose experimental details are shown in **Table 1**, were applied to the material and can be categorized as:

- Additional annealing treatments on heavily cold reduced material (*strain recrystallization*).
- Low cold reduction (applied in tensile mode, 5-15%) plus annealing treatments (*strain annealing*). This treatment type was applied to two different as-received states of the material, solution annealed SA1 and SA2, which exhibited a fully recrystallized microstructure with differences in grain size as well as in precipitation.
- Additional annealing treatments on fully recrystallized material so as to induce *grain growth.*

Table 1 Thermo-mechanical treatments carried out on 18Cr9Ni3CuNbN ASS

Thermo-mechanical treatments	Reduction (%)	Temperature (ºC)	Time (h)
Heavily cold rolled + annealing treatment	~65	1050-1150	0.5-2
Solution annealed + cold reduction + annealing treatment	5-15	950-1200	0.16-24
Solution annealed + additional annealing treatment	-	990-1200	0.5-1

After each annealing treatment, the samples were immediately cooled down in water. Following that, EBSD and FEG-SEM were employed to characterize the samples. The analysis of the HAGB character was analyzed by looking at the low-Σ type boundaries on areas larger than $600 \times 600 \mu m^2$, with a $1 \mu m$ step size. In particular, for the measurements of the coherent $\Sigma 3$ annealing twins, the trace criterion $\{111\}$ –with tolerance lower than 8º– and the $\Sigma 3$ relationship were adopted [1,10]. Moreover, the Kernel Average Misorientation (KAM) parameter was used to define the strain state of the material. The samples were assumed to be strain free material when KAM (third neighbor, 3º) was below 0.5º.

3. Results and discussion

3.1. Effect of the thermo-mechanical treatments on low-Σ boundaries

As a result of applying different thermo-mechanical treatments to this austenitic stainless steel, a wide range of microstructures were generated. The strain annealed samples showed a convoluted grain boundary network, whereas in the samples where only recrystallization and/or grain growth had taken place a more equiaxed HAGB network was attained. The analysis was based on measuring the total CSL boundaries from $\Sigma 3$ to $\Sigma 27$ as the length fraction of the total HAGB (>15º). Some trends can be detected when plotting this fraction as a function of the specific grain boundary area S_v, **Figure 1**.**a**. All the treatments involve a uniform increase in the grain size, and therefore the decrease in S_v, along with the amount of special grain boundaries, except for grain growth treatments at low temperatures and strain annealing treatments under the lowest cold reduction-temperature-time conditions (5%-950/990ºC-<3h). Under such conditions, no effect on the grain boundaries and the microstructural unit size was detected. The highest effectiveness of the strain annealing processes with regard to the other processing routes is fairly evident in terms of the CSL boundary population. In fact, the length fraction of low-Σ boundaries for 5%-990/1030ºC-24h is 85%. This means that the grain boundary network almost reaches the so called twin-limited microstructure in terms of $\Sigma 3$ boundaries [11], since most of the triple points contain two $\Sigma 3$ boundaries. Other austenitic stainless steels for similar combinations of cold reduction-annealing temperatures are able to develop the same low-Σ boundary fraction [6].

Additionally, the microstructural evolution for a fixed strain annealing treatment depends on the as-received recrystallized state, due to the differences in the initial S_v and in precipitation.

As far as the coherent $\Sigma 3$ boundaries are concerned, two readily distinct behaviors are observed when their length fraction is plotted against the fraction of low-Σ boundaries, **Figure 1.b.** Strain recrystallization and pure grain growth treatments at high temperatures (above 1150ºC) slightly enhance the CSL fraction despite the significant increase in coherent $\Sigma 3$ twin boundaries. Conversely, the strain annealing treatments involve the simultaneous increase of CSL and coherent $\Sigma 3$ length fractions. High amounts of $\Sigma 9$ and $\Sigma 27$ were achieved in strain annealed samples -exceeding 9% in most cases- whereas the other samples hardly reached 3%. Regardless of the strategy, the coherent $\Sigma 3$ fraction levels off at the same fraction (~42%) for low S_v. Therefore, the mechanisms responsible for coherent $\Sigma 3$ boundary formation and for $\Sigma 3^n$ type boundary formation are operative when strain annealing treatments are applied. Instead, the mechanism for coherent $\Sigma 3$ boundary formation predominates under recrystallization strain and grain growth treatments at high temperatures.
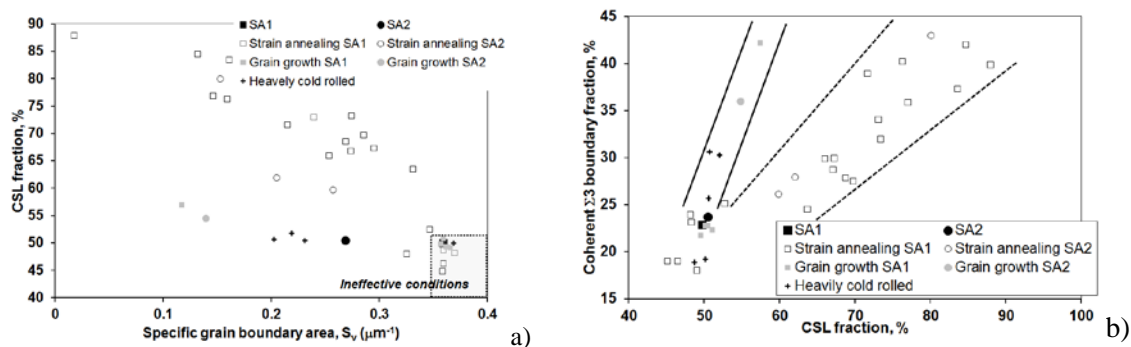

Figure 1 a) Fraction of low-Σ boundaries as a function of the specific grain boundary area. b) Fraction of coherent $\Sigma 3$ annealing twins vs. low-Σ boundary fraction.

### 3.2. Evolution over time of low-Σ boundaries for strain annealing treatments

In order to analyze the development of the special grain boundaries over time, different annealing treatments after a 5% reduction at 990ºC and 1030ºC were carried out for various holding times, **Figure 2.a**. CSL boundary formation kinetics are faster at the highest temperature, 1030ºC, but over time both behaviors converge. The main increase in the amount of special grain boundaries for strain-annealed samples is limited to a time interval in which all the strain energy is largely consumed. After that interval, the amount of Σ boundaries also increases due to subsequent grain growth, but at a much slower rate. A zoom of a region in which strain annealing is effective, after 0.5h at 1030ºC, shows some clues about the generation of the GBCD, **Figure 2.b**. Several strain free regions (black regions, low kernel) are made of a highly twinned microstructure. A few general high angle boundaries in this region appear to be related to the impingement of different highly twinned regions that meet together (arrow between regions A and B).
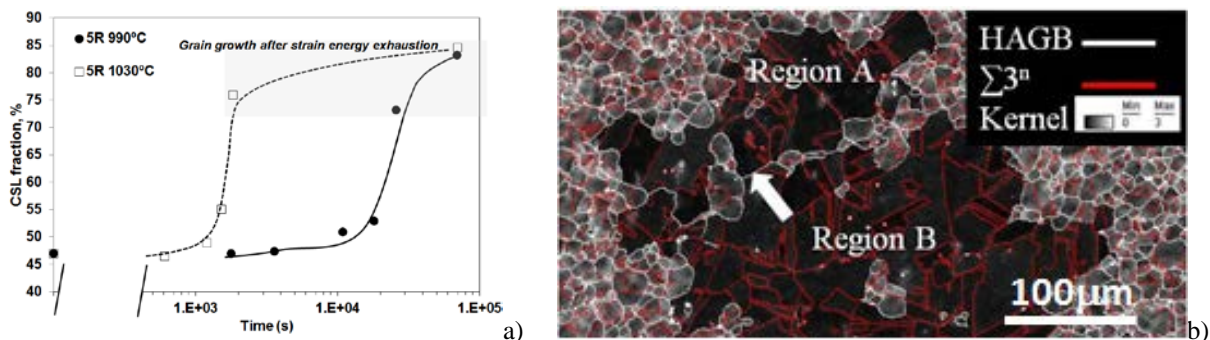
Figure 2 a) Evolution of the CSL fraction over time for a 5% reduction and further annealing (SA1) and **b)** Kernel map with overlapped HAGB network for the 5R-1030ºC-0.5h annealing treatment

3.3. Effect of the precipitation on the low-Σ boundary formation

Precipitation of Nb(C,N) is present in the as-received solution annealed states and during additional annealing treatments. The existence of these precipitates substantially impinges the grain boundary migration, **Figure 3.a**. However, the delaying effect of the precipitation on kinetics does not bring about a noticeable change in the GBCD, as shown by the high fraction of special grain boundaries. This conclusion is also supported by the experimental observations reported for other ASS, where no precipitation was observed at the annealing temperatures but very close fractions of low-Σ boundaries resulted [78-9], **Figure 3.b**, and by a previous theoretical study on particles as a way to control the grain boundary character [12].
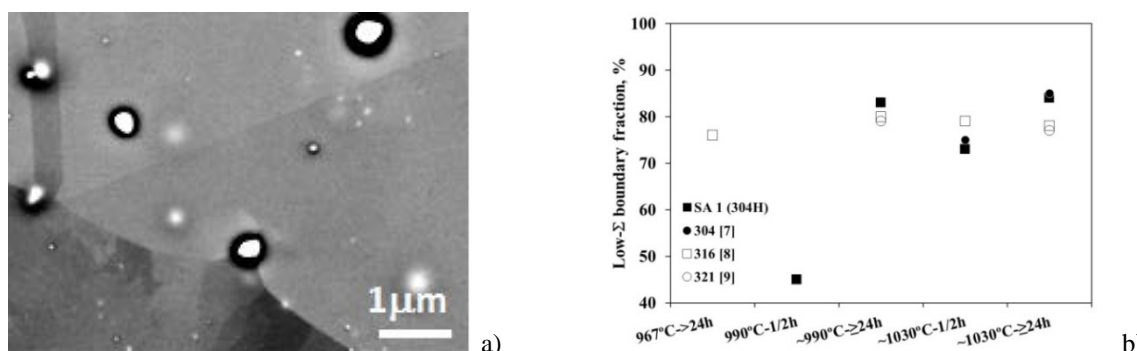
Figure 3 a) Grain boundary migration impingement by Nb(C,N) precipitation and b) low-Σ boundary fraction for different ASS and thermo-mechanical sequences (cold reduction 5%).

4. Conclusions

The evolution of GBCD depending on the thermo-mechanical sequence applied has been tackled in a Nb-stabilized austenitic stainless steel. Recrystallization and/or pure grain grow at temperatures above 1150ºC enhance the formation of annealing twins, whereas strain annealing treatments augment the overall length fraction of low-Σ boundaries. In general, both types of sequences bring about an increase in the grain size. Nb(C,N) precipitation delays the kinetics of the grain boundary migration and its effect on the character of the final grain boundaries appears to be limited. For the time intervals analyzed, further grain growth after strain energy exhaustion involved an increase in the low-Σ boundary fraction in strain annealing treatments.

References

[1]   Brandon D G 1966 *Acta Metall.* **14** 1479
[2]   Randle V 2006 *Scripta Mater.* **54** 1011
[3]   Randle V 2004 *Acta Mater.* **52** 4067
[4]   Kumar M, King W E and Schwartz A J *Acta Mater.* 2000 **48** 2081
[5]   Beddoes J and Parr J G 1999 *Introduction to Stainless Steels*, ASM International, OH (USA)
[6]   Fang X, Zhang K, Guo H, Wang W and Zhou B *Mater. Sci. Eng. A* 2008 **487** 7
[7]   Shimada M, Kokawa H, Wang Z J, Sato Y S and Karibe I 2002 *Acta Mater.* **50** 2331
[8]   Michiuchi M, Kokawa H, Wang Z J, Sato Y S and Sakai K 2006 *Acta Mater.* **54** 5179
[9]   Kurihara K et al. 2011 *J. Mater. Sci.* **46** 4270
[10] Randle V, Davies H 2002 *Ultramicroscopy* **90** 153
[11] Palumbo G et al. *Phys. Stat. Sol.* 1992 **131** 425
[12] Miodownik M A 2006 *Scripta Mater.* **54** 993